09

A computer algebra application for the solution of the ray tracing problem

© V. Pauls, A.A. Tchertovskikh

Institute for Physics of Microstructures of the Russian Academy of Sciences GSP-105,
603950 Nizhny Novgorod, Russia
e-mail: walter.pauls@gmail.com

Received May 28, 2025
Revised May 28, 2025
Accepted May 28, 2025

For X-ray optics with mirrors described by second-order surfaces, raytracing can be performed explicitly. Two types of the Schwarzschild configuration are considered — a configuration with nonconcentric spherical mirrors and a configuration where the first mirror is a spheroid. The obtained exact solutions were analyzed using symbolic algebra systems, which, in some cases, enables us to calculate higher order aberrations, such as all fifth-order aberrations. For the Schwarzschild scheme with spherical mirrors, it was shown that the approximating solutions converge well to the exact ones. For the scheme with one elliptical mirror, we caclulated the third-order aberrations and analyzed the conditions for aplanaticity.

Keywords: X-ray optics, Schwarzschild configuration, elliptical mirror, ray tracing, aberrations, symbolic algebra.

DOI: 10.61011/TP.2025.10.62077.113-25

Introduction

Due to a significant progress in multilayer mirror coating technology (see, for example, the tables with record-breaking reflection coefficients in [1,2]), reflective X-ray optics are gaining ground, ranging from applications in X-ray microscopy and lithography to X-ray astronomy. X-ray optical configurations have their own particularities. Even for record-breaking reflection coefficients of multilayer mirrors in the X-ray wavelength range such as 72% at $\lambda = 11.2\,\text{nm}$, effective radiation intensity drops rapidly (exponentially) as the number of mirrors increases. Thus, the number of employed mirrors is strictly limited. Another feature of X-ray optics is a high level of requirements for permissible mirror surface deviations from the specified profile due to short operating wavelength, for example, shorter than $\lambda/14$ by the Marechal criterion. Fabrication and metrology of mirrors with large deviations from a spherical shape at this level require huge expenditures and present severe difficulties [3]. Finally, note that multilayer mirrors for normal incidence optics do not permit large incidence angle variations because of the need to satisfy the Bragg-Wulff condition.

Thus, unlike optical configurations for wavelengths up to deep ultraviolet, mirror X-ray configurations in most cases have a relatively simple configuration. This may be illustrated by a double-mirror Schwarzschild configuration that uses two spherical mirrors in its simplest version. In such situation from a theoretical standpoint, it is absolutely appropriate to ask the question which properties of simple mirror systems can be explicitly described without using numerical simulations. Analytical calculations of the Schwarzschild configuration properties were performed in [4–7] for concentric and nonconcentric configurations. These studies determined third order and fifth order spherical aberrations, also, third order Seidel aberrations were obtained at aplanatic points. Study [7] proposes using the smallest diameter of the focal spot on the optical axis as design merit function.

The purpose of this work is to develop a systematic approach to the analysis of simple mirror configurations within raytracing optics based on the following observations:

- during raytracing, the point of intersection between a ray and a given quadric surface may be found explicitly;
- tracing uses recursive definition of image maps describing the transfer of beam configurations between surfaces;
- computer algebra allows us to work with bulky expressions which otherwise we would not be able to processed manually.

Thus, for a low number of mirrors, for example, one or two, explicit expressions for an optical configuration of rays reflected from the object plane to the image plane can be derived. Expressions of this kind may be further used to evaluate the accuracy of numerical tracing methods, to analyze the dependence of Seidel aberrations on optical configuration parameters, for preliminary improvement of optical configurations, et cetera.

Section 1 will describe in detail the method that we used for analytical raytracing. Section 2 will address the well-known Schwarzschild double-mirror configuration with spherical mirrors, high order aberrations will be calculated, including the fifth order ones, and convergence of paraxial expansion to the exact solution will be discussed. Section 3 will deal with the Schwarzschild configuration where the first mirror is a spheroid, and an attempt will be made to evaluate whether the ensuing increase in the number of degrees of freedom for optical configuration assignment makes it possible to improve the optical imaging quality.

1. An analytical ray tracing method

It is known that the problem of raytracing through an optical system within raytracing optics reduces to sequential calculation of the condition for a ray to intersect an optical surface, and to determining the reflected or refracted ray direction. For convenience, an optical ray configuration will be considered using the Hamiltonian formalism (see §18 of [8]). It is always implied that the refractive index of a medium is equal to 1. Suppose the object plane is parallel to the xy plane and intersects the z axis at point z_{Obj}. Assume that the analyzed ray goes from point $\mathbf{r}^{(0)} = (x, y, z_{Obj})$ in a direction set by a unit vector (directing vector) $\hat{\mathbf{d}}^{(0)} = (p, q, \sqrt{1-p^2-q^2})$ (ray direction in spherical coordinates can be also written as $\hat{\mathbf{d}}^{(0)} = (\sin\alpha\cos\beta, \sin\alpha\sin\beta, \cos\alpha)$). Note that the ray configuration is fully defined by the vector$\omega = (x, y, p, q)$. The ray itself up to the point of intersection with the following optical surface is described as $\mathbf{r}^{(0)} + t\hat{\mathbf{d}}^{(0)}$.

For tracing from the optical surface i to the optical surface $i+1$, it is necessary to: a) calculate the point of intersection $\mathbf{r}^{(i+1)}$ of the ray $\mathbf{r}^{(i)} + t\hat{\mathbf{d}}^{(i)}$ with the next optical surface, b) for a ray reflected from a mirror calculate the reflected ray direction $\hat{\mathbf{d}}^{(i+1)}$. Suppose that the optical surface equation is given implicitly as $F(\mathbf{r}) = 0$, where $\mathbf{r} = (x, y, z)$. Then the point of intersection between the ray and surface is found using solution t^* (not necessarily the only one) to

$$F(\mathbf{r}^{(i)} + t^*\hat{\mathbf{d}}^{(i)}) = 0, \tag{1}$$

as $\mathbf{r}^{(i+1)} = \mathbf{r}^{(i)} + t^*\hat{\mathbf{d}}^{(i)}$. To find the reflected ray direction using

$$\hat{\mathbf{d}}^{(i+1)} = \hat{\mathbf{d}}^{(i)} - 2\langle\hat{\mathbf{d}}^{(i)}, \hat{\mathbf{n}}^{(i+1)}\rangle\,\hat{\mathbf{n}}^{(i+1)} \tag{2}$$

, normal direction $\hat{\mathbf{n}}^{(i+1)}$ to the mirror at point $\mathbf{r}^{(i+1)}$ shall be known and is calculated as the gradient of $F(x, y, z)$. Note that both $\hat{\mathbf{d}}^{(i)}$ and $\hat{\mathbf{n}}^{(i)}$ are unit vectors.

In some cases equation (1) defining the point of intersection can be solved explicitly. Specifically, explicit solutions are possible at least theoretically provided that $F(x, y, z)$ is a polynomial not higher than the fourth degree. Since the explicit expressions for solutions to the fourth degree equations are extremely cumbersome, we currently limit ourselves to addressing the following surface of rotation about the z axis not higher than the second order:

- spherical surface

$$F(x, y, z) = x^2 + y^2 + z^2 - R^2,$$

- spheroid

$$F(x, y, z) = \frac{x^2}{a^2} + \frac{y^2}{a^2} + \frac{z^2}{b^2} - 1,$$

- two-sheeted hyperboloid of revolution

$$F(x, y, z) = \frac{x^2}{a^2} + \frac{y^2}{a^2} - \frac{z^2}{b^2} + 1,$$

- spherical paraboloid

$$F(x, y, z) = \frac{x^2}{a^2} + \frac{y^2}{a^2} - 2z.$$

Note that the above mentioned forms of optical surfaces may be reduced to a more convenient form, if desired, by shifting the coordinate system. Another consideration in favor of limiting the order of optical surface is reduction of uncertainty induced, in the case of a high order surface, by the need to choose one of several solutions to equation (1).

Raytracing is generally performed from an object plane to an image plane that is also assumed parallel to the xy plane and intersecting the z axis at point z_{Img}. Points of intersection with mirrors and reflected ray directions are calculated recursively. Assuming that the optical surface with index i is the last, from which the ray is reflected before intersecting the image plane, the following expression is derived for point $\mathbf{r}^{(Img)}$ where the ray intersects the image plane:

$$\mathbf{r}^{(Img)} = \mathbf{r}^{(i)} + \frac{z_{Img} - r_z^{(i)}}{\hat{d}_z^{(i)}}\,\hat{\mathbf{d}}^{(i)}.$$

Here, $r_z^{(i)}$ and $\hat{d}_z^{(i)}$ denote the $\mathbf{r}^{(i)}$ and $\hat{\mathbf{d}}^{(i)}$ projections to the z axis. Note that $\hat{\mathbf{d}}^{(Img)}$ of the ray intersecting the image plane coincides with $\hat{\mathbf{d}}^{(i)}$ of the beam reflected from the last optical surface. Since the optical ray configuration is described by coordinates of the point of intersection between the ray and the(P, Q) plane on the x and y axes, we get a description of the optical image $\Omega(x, y, p, q) : \mathbb{R}^4 \longrightarrow \mathbb{R}^4$ as consisting of four functions $X(x, y, p, q)$, $Y(x, y, p, q)$, $P(x, y, p, q)$, $Q(x, y, p, q)$. For axisymmetric systems, image $\Omega(x, y, p, q)$ is invariant with respect to rotations about the z axis. Moreover, since the given system is Hamiltonian, the phase volume is preserved. Both requirements impose significant limitations on possible optical images. Note that, when calculating lens systems, all remarks concerning the calculation of points of intersection between the ray and optical surfaces using equation (1) remain valid and reflection law (2) shall be replaced with Snell's law. Expressions derived for lens systems in this case are more cumbersome due to a higher algebraic complexity of the Snell equation and the presence of two optical surfaces in a single lens.

Despite an apparent simplicity of the above-mentioned approach, the explicit expressions for the optical configuration of the traced ray become so cumbersome after one to two steps that manual processing is virtually impossible any longer. For such expressions, computer algebra systems such as Mathematica [9] (used for this work), Maple, and recently developed Symbolica may be used. Some examples of using such systems are discussed below. The final section will contain conclusions and generalization of the method used in this work for general mirrors.

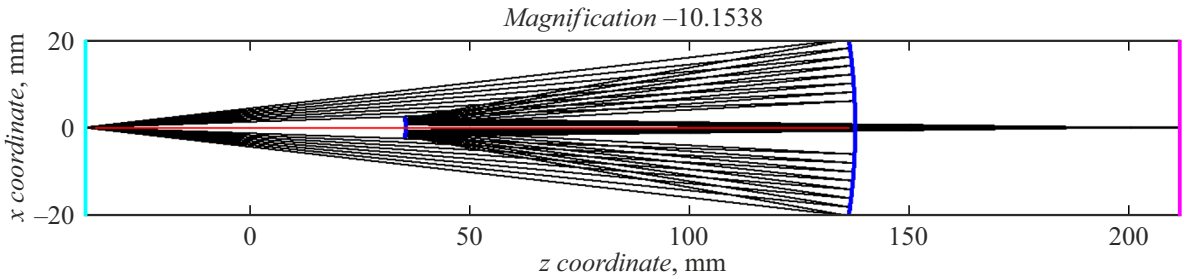

Figure 1. Schwarzschild configuration with two spherical mirrors. Radius of the first concave mirror $R_1 = 137.5$ mm, radius of the second convex mirror $R_2 = 24$ mm. Center-to-center distance between the first and second mirrors $m = 11.5$ mm. The object plane $z_{Obj} = -37.5$ mm is cyan, the image plane $z_{Obj} \approx 211.8077$ mm is purple.

2. Schwarzschild configuration with spherical mirrors

Schwarzschild configuration (Figure 1) with two spherical mirrors is one of the best understood optical mirror systems in the X-ray optics.

To simplify our configuration, the first concave mirror is assumed to be centered at the origin of coordinates. For simplicity, we follow [7] and assume that the radius of the second convex mirror is equal to 1, while the radius of the first concave mirror is set as a free parameter R. Since the analyzed configuration is not necessarily concentric, the center of the second mirror is on the z axis at point $z = m$. Note that computer algebra can be used to give explicit expression for an optical image. Due to their bulkiness, expressions for $\mathbf{r}_x^{(Img)}$, $\mathbf{r}_y^{(Img)}$, $\mathbf{r}_z^{(Img)}$ and $\hat{\mathbf{d}}_x^{(Img)}$, $\hat{\mathbf{d}}_y^{(Img)}$, $\hat{\mathbf{d}}_z^{(Img)}$ were stored as 50KB and 83 KB *.m* ASCII text files (Mathematica batch file). At this point, it seems that such explicit expressions may be used only to check the calculation accuracy of numerically simulated optical configurations. Nevertheless, for design of optical configurations of X-ray lithography projection lenses, approaches were proposed [10,11] where configurations with spherical mirrors were used for rough estimate of the optical and design parameter space. Utilized as initial conditions for further improvement using aspherical corrections, they may make it possible, due to the smallness of corrections, to determine such parameters as mirror sizes and positions. One may hope that exact solutions will provide better evaluation of the optical image quality for such initial configurations.

To get more detailed information, we resort to Taylor's series expansion of the optical image $\omega(x, y, p, q)$ in(x, y, p, q):

$$\Omega(x, y, p, q) = \sum_{n_x=0}^{\infty}\sum_{n_y=0}^{\infty}\sum_{n_p=0}^{\infty}\sum_{n_q=0}^{\infty}\Omega(n_x, n_y, n_p, n_q)x^{n_x}y^{n_y}p^{n_p}q^{n_q}, \tag{4}$$

where

$$\Omega(n_x, n_y, n_p, n_q) = \frac{1}{n_x!n_y!n_p!n_q!}\frac{\partial^{n_x}}{\partial x^{n_x}}\frac{\partial^{n_y}}{\partial y^{n_y}}\frac{\partial^{n_p}}{\partial p^{n_p}}\frac{\partial^{n_q}}{\partial q^{n_q}} \times \Omega(x, y, p, q)|_{(x,y,p,q)=0}.$$

Since, due to the axial symmetry, all even-degree terms are equal to zero, the first order terms will be calculated first. Paraxial focus position with respect to z can be found by setting, for example, the derivative of $X(x, y, p, q)$ with respect to p to zero and getting the following expression:

$$z_{parax} = \frac{2mR + 2m^2R - 4mz_{Obj} - 4m^2z_{Obj} + Rz_{Obj} + 2mRz_{Obj}}{R + 2mR - 2z_{Obj} - 4mz_{Obj} + 2Rz_{Obj}}. \tag{5}$$

Then the first order derivative matrix at point $(x, y, p, q) = 0$ will be given by

$$\begin{pmatrix} \partial_x X & \partial_y X & \partial_p X & \partial_q X \\ \partial_x Y & \partial_y Y & \partial_p Y & \partial_q Y \\ \partial_x P & \partial_y P & \partial_p P & \partial_q P \\ \partial_x Q & \partial_y Q & \partial_p Q & \partial_q Q \end{pmatrix} = \begin{pmatrix} \frac{1}{\mathfrak{a}} & 0 & 0 & 0 \\ 0 & \frac{1}{\mathfrak{a}} & 0 & 0 \\ \mathfrak{b} & 0 & \mathfrak{a} & 0 \\ 0 & \mathfrak{b} & 0 & \mathfrak{a} \end{pmatrix} + \Delta z \begin{pmatrix} \mathfrak{b} & 0 & \mathfrak{a} & 0 \\ 0 & \mathfrak{b} & 0 & \mathfrak{a} \\ 0 & 0 & 0 & 0 \\ 0 & 0 & 0 & 0 \end{pmatrix}, \tag{6}$$

where $\mathfrak{a}$ and $\mathfrak{b}$ are defined as

$$\mathfrak{a} = \frac{R + 2mR - 2z_{Obj} - 4mz_{Obj} + 2Rz_{Obj}}{R},$$

$$\mathfrak{b} = \frac{2 + 4m - 2R}{R}.$$

Δz denotes the distance from the paraxial focus to the image plane $\Delta z = z - z_{parax}$. Note that the foregoing equations can be easily derived using matrix optics [12], while to calculate higher order aberrations, it becomes necessary to use computer algebra.

For the Schwarzschild configuration with spherical mirrors, calculation of derivatives using Mathematica on Intel Core i5-1235U 16 GB computer takes several minutes, while its takes several hours to calculate all fifth order derivatives. Therefore, higher order derivatives up to the eleventh order have been calculated only for spherical aberration and distortion, because calculation complexity grows very rapidly as the order of derivatives increases. For some eleventh order aberrations, calculation takes several hours.

Since the Schwarzschild configuration is axisymmetric and invariant with respect to reflections, all allowable third order derivatives are described by twelve real parameters. In addition, $\Omega(x, y, p, q)$ preserves the phase volume, which reduces the number of free parameters to six. Five of them define components $X(x, y, p, q)$ and $Y(x, y, p, q)$ and correspond to the Seidel aberrations. Since general expressions for the nonconcentric Schwarzschild configuration turn out to be too bulky, we limit ourselves to giving here expressions for spherical aberration

$$A = -\frac{(R-1)z_{Obj}^2}{R^2 f(R, z_{Obj})} \times \left(R^2(z_{Obj}+1)^2 - R(2+3z_{Obj})z_{Obj} + z_{Obj}^2\right),$$

coma

$$B = \frac{3(R-1)z_{Obj}}{R^2 f(R, z_{Obj})} \times \left(R^2(z_{Obj}+1)^2 - R(2+3z_{Obj})z_{Obj} + z_{Obj}^2\right),$$

field curvature C

$$C = -\frac{R-1}{R^2 f(R, z_{Obj})}\left(R^2(1+4z_{Obj}+2z_{Obj}^2) - 2R(2+3z_{Obj})z_{Obj} + 2z_{Obj}^2\right),$$

astigmatism D

$$D = -\frac{R-1}{R^2 f(R, z_{Obj})} \times \left(R^2(z_{Obj}+1)^2 - R(2+3z_{Obj})z_{Obj} + z_{Obj}^2\right),$$

and distortion E

$$E = -\frac{R-1}{R^2 f(R, z_{Obj})} \times \left(R(2+3z_{Obj}) - R^2(z_{Obj}+2) - z_{Obj}\right),$$

in the paraxial focus plane for the concentric configuration $m = 0$. In the foregoing expression $f(R, z_{Obj}) = (R - 2z_{Obj} + 2Rz_{Obj})$. From the expression for spherical aberration, well known conditions for aplanatic points are obtained. These conditions also generally turn out to be very bulky and therefore are not given here. Note that it follows from the foregoing relations that, for the concentric Schwarzschild configuration at aplanatic points,

$$z_{Ob}^{(+)} = -\frac{R}{R+\sqrt{R}-1},$$

$$z_{Ob}^{(-)} = -\frac{R}{R-\sqrt{R}-1},$$

spherical aberration, coma and astigmatism are simultaneously equal to zero, and for field curvature and distortion, we get

$$C^{(+)} = -\frac{(R-1)(R+\sqrt{R}-1)}{R(R-\sqrt{R}-1)},$$

$$C^{(-)} = -\frac{(R-1)(R-\sqrt{R}-1)}{R(R+\sqrt{R}-1)},$$

and

$$D^{(+)} = -\frac{(R-1)(R+\sqrt{R}-1)^2}{R^2(R-\sqrt{R}-1)},$$

$$D^{(-)} = -\frac{(R-1)(R-\sqrt{R}-1)^2}{R^2(R+\sqrt{R}-1)}.$$

Expressions for the fifth order spherical aberration are also given for reference

$$A^{(+)} = \frac{3(R-1)^3R^2}{4(R-\sqrt{R}-1)(R+\sqrt{R}-1)^5},$$

$$A^{(-)} = \frac{3(R-1)^3R^2}{4(R-\sqrt{R}-1)^5(R+\sqrt{R}-1)}.$$

To evaluate the degree of applicability of power series expansions when addressing optical configurations, numerical results obtained from ray tracing which use explicit expressions for an optical image are compared with approximate calculations, including aberrations higher than the third order. Results of ray tracing using explicit expressions in turn were checked in Zemax. Figure 2 shows the results of spherical aberration and distortion comparison.

It can be seen from the comparison with the exact solution that, as the approximation order increases, the difference between the exact and approximate solutions decreases. For example, for the spherical aberration shown on the left in Figure 2, agreement between the exact and approximate solutions seems to be quite good up to the aperture approximately equal to $0.4 - 0.5$ for the fifth and seventh orders. It is expected that, with systematic increase in the order, approximations will converge to the exact solution because Figure 3 shows that the difference between exact and approximate solutions apparently decreases as the approximation order increases from the third to eleventh. Though the order of calculated aberrations is too low to draw conclusions about the convergence rate and behavior of the corresponding Taylor's power series (according to the experience of power series analysis in statistical physics, approximately one hundred coefficients are required for this), nevertheless, it seems that, at least in the studied configuration, this series behaves quite well.

Summing up the study of the Schwarzschild configuration with spherical mirrors, it can be said that computer algebra methods provide an exhaustive analysis of this configuration due to its simplicity. At the same time, the space of possible parameters is too limited to allow for comprehensive design. The nonconcentric configuration with spherical mirrors and fixed magnification allows for only one free parameter — center-to-center distance between mirrors. Another degree of freedom for the configuration design may be introduced using a spheroid instead of a sphere for the first concave mirror, which will be done in Section 3.

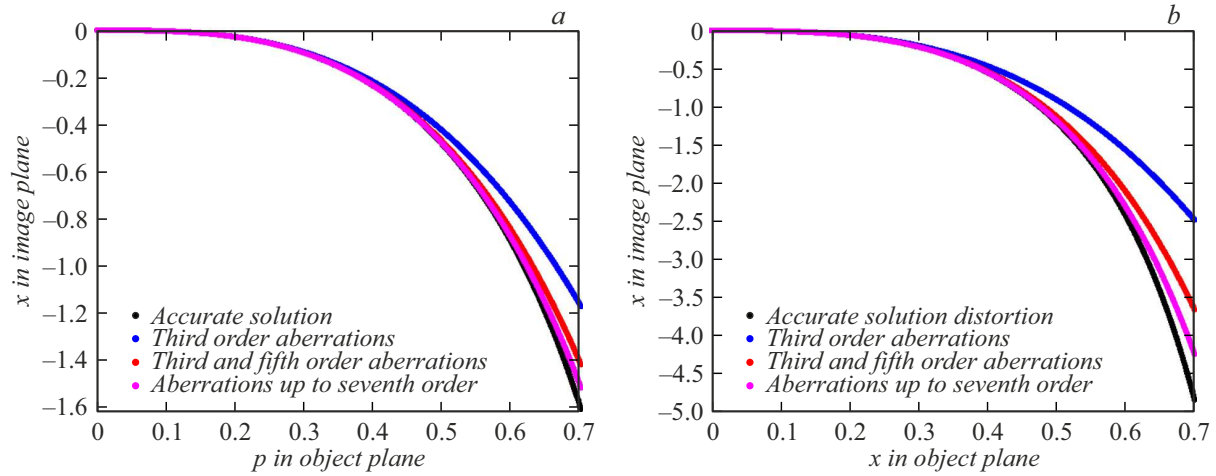

Figure 2. Comparison of exact ray tracing with third, fifth and seventh order approximations for the Schwarzschild configuration with the same parameters as in Figure 1. For clarity, coordinates are normalized with respect to the radius of the second mirror. Comparison for rays coming from a point on the z axis with directions on the xz plane, i.e. with the initial configuration $(0, 0, p, 0)$, is shown on the left. Comparison for rays parallel to the z axis from a point on the x axis, i.e. with the initial configuration $(x, 0, 0, 0)$, is shown on the right. To facilitate the comparison, a part corresponding to linear increase was subtracted from the exact solution so that only nonlinear distortion can be seen

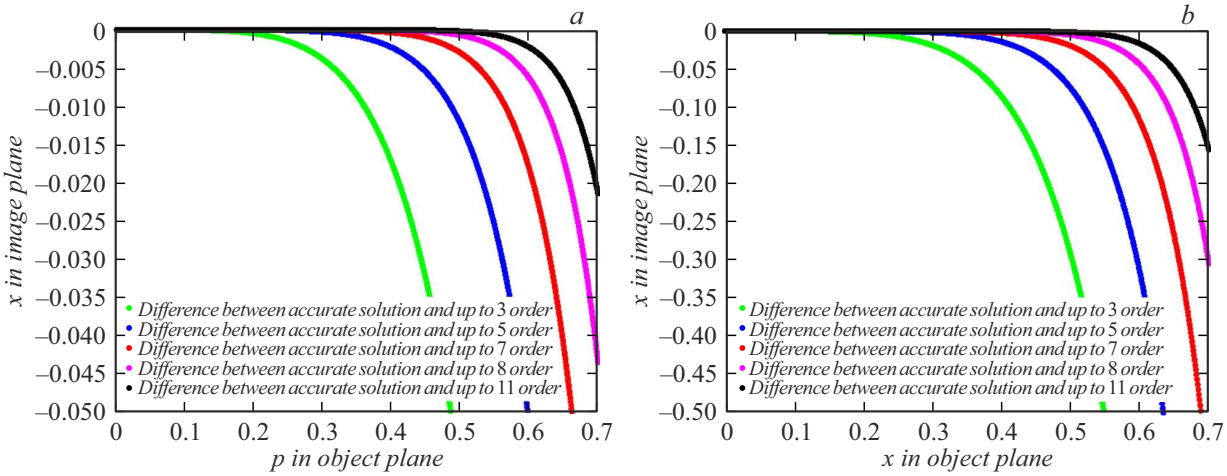

Figure 3. Numerical difference between exact ray tracing and approximations up to the third, fifth, seventh, ninth and eleventh orders for the Schwarzschild configuration with the same parameters as in Figure 1. Unlike Figure 2, discrepancy between the exact and approximate solutions is shown. For clarity, coordinates are normalized with respect to the radius of the second mirror. Results for rays going from a point on the z axis with directions on the xz plane, i.e. with the initial configuration $(0, 0, p, 0)$, are shown on the left. Results for rays parallel to the z axis from a point on the x axis, i.e. with the initial configuration $(x, 0, 0, 0)$, are shown on the right.

3. Schwarzschild configuration with one spherical mirror and one spheroid mirror

Since explicit ray tracing is also possible, for example, for spheroids, a double-mirror Schwarzschild configuration was examined where the first concave mirror is a spheroid with a and b. Despite a seemingly minor change in the optical configuration, the problem complexity (in terms of the amount of calculation) grows more than by an order of magnitude. Thus, the size of ASCII text files with exact expressions for $\mathbf{r}_x^{(Img)}$, $\mathbf{r}_y^{(Img)}$, $\mathbf{r}_z^{(Img)}$ and $\hat{\mathbf{d}}_x^{(Img)}$, $\hat{\mathbf{d}}_y^{(Img)}$, $\hat{\mathbf{d}}_z^{(Img)}$ is now 1091KB and 657 KB.

Due to the growing complexity of expressions, at this point we limit ourselves to the calculation of first order quantities such as paraxial focus,

$$z_{parax} = \frac{h(a, b, m, z_{Obj})}{g(a, b, m, z_{Obj})}$$

first derivative matrix, third order aberrations, calculation of which took several hours. The first derivative matrix has the same form as in equation (6), the only difference being that $\mathfrak{a}$ and $\mathfrak{b}$ are given this time as

$$\mathfrak{a} = \frac{a^2}{g(a, b, m, z_{Obj})},$$

$$\mathfrak{b} = 2 + \frac{2b(2m - 2b + 1)}{a^2}.$$

In the foregoing equations, $g(a, b, m, z_{Obj})$ and $h(a, b, m, z_{Obj})$ are polynomials in the variables$a$, b, m, z_{Obj} given by

$$g(a, b, m, z_{Obj}) = 2b(-1 + 2b - 2m)(b - z_{Obj}) + a^2(1 - 4b + 2m + 2z_{Obj}),$$

and

$$h(a, b, m, z_{Obj}) = 2b(b + 2bm - 2m(1 + m))(b - z_{Obj}) + a^2(2m^2 - 2b(1 + 2m) + z_{Obj} + 2m(1 + z_{Obj})).$$

explicit expressions for the third order aberrations are so bulky that it was considered unsuitable to give them here. Nevertheless, calculation results for the Schwarzschild configuration with spherical mirrors and configurations with one elliptical mirror were grouped in the form of a Mathematica batch and are publicly available at gitflic website.

When dealing with optical configurations with a fixed magnification M, additionally applying the aplanatic condition, then the space of solutions will be two-dimensional in contrast to the Schwarzschild configuration with concentric spherical mirrors. As an example, a configuration with tenfold magnification was evaluated by varying a and m. m was varied from -1 to 1, while a was varied from $R^* - 1$ to $R^* + 1$, where

$$R^* = \frac{3 + 2M + 3M^2 - (M - 1)\sqrt{5 + 6M + 5M^2}}{2(1 + 2M + M^2)}$$

is the radius corresponding to the tenfold magnification in the concentric Schwarzschild configuration with spherical mirrors. Figure 4 shows the variation of positions of the object plane and paraxial focus plane on a and m. b is calculated in this case from the aplanatic condition and fixed magnification.

To evaluate the optical configuration quality, corresponding variations of the third order aberrations as shown in Figure 5 were also calculated. The figure shows that the aplanatic point of the concentric configuration is the only one where coefficients of simultaneously three third order aberrations disappear — spherical aberration, coma and astigmatism. In addition, it can be seen that the field curvature and distortion coefficients vary differently in different directions when a and m are varied, so there is no obvious configuration other than concentric where both coefficients are optimal. Thus, for further optimization of the Schwarzschild configuration, surfaces with order higher than the second one have to be considered.

Conclusions

The study has shown that simple optical configurations using mirrors described by second order surfaces can be analyzed in detail using software packages for symbolic computation. For the Schwarzschild configuration with spherical mirrors, all aberrations up to the fifth order, including, and partially some aberrations up to the eleventh order have been determined. Numerical simulation has been used to show that the approximate solutions adequately converged to the exact solutions, holding out a hope of extending the scope of application of paraxial expansions provided that we would be in position to calculate higher orders. Note that the approach used in this work is also applicable to the review of optical lens configurations. For chromatic aberration calculation, the aberration calculation procedure based on Taylor's series expansions also needs to include a wavelength dependence.

The concentric Schwarzschild configuration is known to permit two aplanatic configurations or fixed magnification, which considerably limits the number of allowable optical configurations. The number of degrees of freedom may be increased by using nonconcentric configurations and replacing the first spherical mirror by a spheroid. For such systems, third order aberrations were calculated and the effects of mirror center-to-center distance variation and deviation from spherical shape were investigated.

In this case, it turned out that an increase in the number of degrees of freedom didn't give any significant results because coma and astigmatism also disappear at the aplanatic points of the concentric Schwarzschild configuration. It is commonly known that high order aspherical corrections are used in practice to improve the image quality in the Schwarzschild configuration. Therefore, it is reasonable to ask whether the approach used in the work may be extended to mirrors with an order higher than the second one.

As noted in Section 1, explicit ray tracing, from theoretical standpoint, may be performed only for surface not higher than the fourth order. Thus, the approach addressed in the work will not be generally applicable. In addition, the approach based on applicability of explicit solutions turns out to be quite wasteful in terms of computation, because, in the analysis based on the consideration of aberrations, albeit of very high order, we use only a small part of all available information about solutions, i.e. some limited number of derivatives. Nevertheless, an alternative approach is possible, which will be described here only in broad terms and considered in greater detail in next publications. It is based on two observations: first, matrix optics that describes first order effects may be generalized so that it includes arbitrary order aberrations, second, for individual mirrors, high order aberrations may be determined by calculating derivatives of implicit functions.

Note that extensions of the matrix approach in the electron and ion optics for calculation of second order aberrations were proposed as early as in the 1960s (see [13,14]), however, as far as we know, this approach was not generalized and systematized. The developed generalization proposes to describe an optical image map from one plane to another using the so-called matrix representation of the

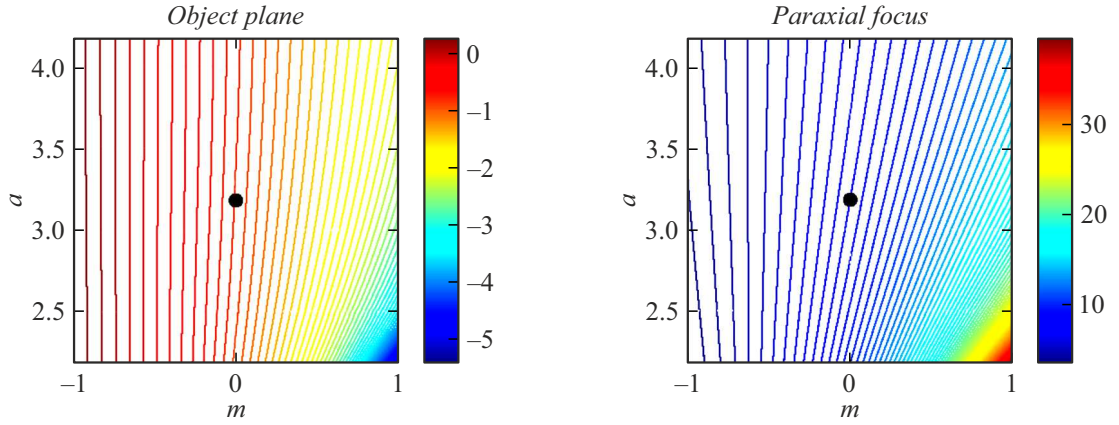

Figure 4. Dependence of positions of the object plane z_{Obj} and paraxial focus plane on a and m while simultaneously fulfilling the aplanatic condition. Black point indicates the aplanatic point for the concentric Schwarzschild configuration with spherical mirrors

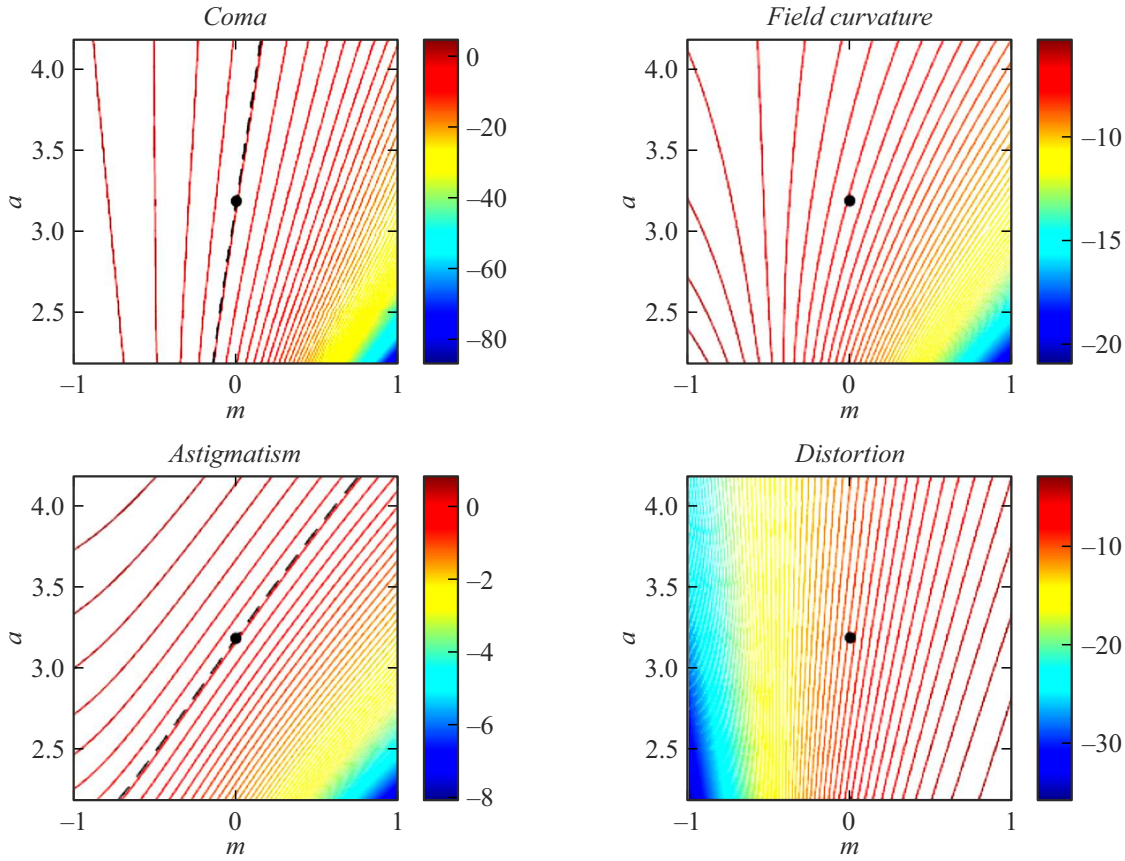

Figure 5. Dependence of coma, field curvature, astigmatism and distortion on a and $m$obeying the aplanatic condition. Black point corresponds to the aplanatic point for the concentric Schwarzschild configuration with spherical mirrors. Dashed line shows coma and astigmatism zero levels.

group of formal diffeomorphisms where a composition of images is represented by means of matrix multiplication (for 1D case, such a representation was given in [15]). The computation of an optical scheme can be performed in this case by determining aberrations of the optical image map from one plane to another, where the planes are properly arranged between the mirrors, and constructing the resulting image map from the object plane to the image plane as a recursively determined composition of image maps.

Finally, note that the representation of the optical image map in the form of a series expansion, such as (4) can be also used to evaluate the point spread function, given the numerical aperture, as it was done in [7]. However, in contrast to the mentioned work, the point spread function

in our case can be also calculated in off-center position in dependence on the field coordinate. This aspect is particularly important in view of the fact that the Schwarzschild type configurations have nonzero obscuration.

Funding

Algorithms were developed within state assignment № FFUF-2024-0022, numerical calculations were supported by grant of the Russian Science Foundation № 21-72-30029-P. The authors are grateful to the reviewers for their useful comments.

Conflict of interest

The authors declare no conflict of interest.

References

[1] V.N. Polkovnikov, N.N. Salashchenko, M.V. Svechnikov, N.I. Chkhalo. UFN, **190**, 92 (2020) (in Russian). DOI: 10.3367/UFNr.2019.05.038623
[2] V. N. Polkovnikov, N. I. Chkhalo. Tez. dokl. XXIX simpoziuma „*Nanofizika i nanoelektronika*“ (N. Novgorod, Russia, 2025), s. 533 (in Russian).
[3] P. Graeupner, P. Kuerz. Proc. SPIE, 12051, 1205102 (2022). DOI: 10.1117/12.2614778
[4] D.L. Shealy, D.R. Gabardi, R.B. Hoover, A.B. Walker Jr., J.F. Lindblom, T.W. Barbee Jr. J. Xray Sci. Technol., **1**, 190 (1989). DOI: 10.3233/XST-1989-1207
[5] A.A. Malyutin, Quantum Electron., **27** (1), 90 (1997). DOI: 10.1070/QE1997v027n01ABEH000801
[6] I.A. Artioukov, K.M. Krymski. Opt. Eng., **39** (8), 2163 (2000). DOI: 10.1117/1.1303727
[7] A. Budano, F. Flora, L. Mezi. Appl. Opt., **45** (18), 4254 (2006). DOI: 10.1364/AO.45.004254
[8] R.K. Luneburg. *Mathematical Theory of Optics* (University of California Press, Berkeley and Los Angeles, 1966)
[9] Wolfram Research, Inc., Mathematica, 14.1, 2024.
[10] F. Liu, Y. Li. Opt. Rev., **20** (2), 120 (2013). DOI: 10.1007/s10043-013-0017-2
[11] F. Liu, Y. Li. Appl. Opt., **52**(29), 7137 (2013). DOI: 10.1364/AO.52.007137
[12] A. Gerrard, J.M. Burch. *Introduction to Matrix Methods in Optics* (A Wiley-Interscience Publication, London NY Sydney Toronto, 1975)
[13] K.L. Brown, R. Belbeoch, P. Bounin. Rev. Sci. Instrum., **35**, 481 (1964). DOI: 10.1063/1.1718851
[14] I. Takeshita. Z. Naturforschg., **21** (1–2), 9 (1966). DOI: 10.1515/zna-1966-1-204
[15] A. Frabetti, D. Manchon. *IRMA Lect. In Math. And Theor.* Phys., (K. Ebrahimi-Fard et F. Fauvet eds), v. 21, p. 91–148. Europ. Math. Soc. (2015).

Translated by E.Ilinskaya